A new kinetic model for the acid-catalysed reactions of *N*-(2-aminophenyl)phthalamic acid in aqueous media

Christopher J. Perry

School of Applied Sciences, University of Wolverhampton, UK WV1 1SB

The acid-catalysed breakdown of *N*-(2-aminophenyl)phthalamic acid has been studied in dilute aqueous acids in the pH range 0–6. The dominant reaction is the formation of *N*-(2-aminophenyl)phthalimide (between ~80 and ~100% yields in the pH range studied) and its subsequent rearrangement to 2-(2-carboxyphenyl)benzimidazole, occurring as consecutive pseudo-first-order processes. Anomalously, only a minor hydrolysis reaction is observed.

A kinetic model for these processes has been constructed and rate constants and activation parameters evaluated. Mechanisms involving pre-equilibria to form the kinetically significant species have been proposed for the consecutive processes. The approach has been adapted to account for the observed kinetics of acid catalysed formation of benzimidazoles from *o*-aminoanilides.

Introduction

There has been considerable interest in the chemistry of *N*-(2-aminophenyl)phthalamic acid[1–5] (**1a**≡**A**) particularly in the study of models for the linkages found in pyrrone ladder polymers. Prior to this study, the kinetics and mechanisms of the intramolecular reactions of **1a** did not appear to have been investigated in detail in dilute aqueous media. Hawkins[6] has shown that for a range of substituted phthalanilic acids (**1** with X = either 3′ or 4′ -Cl, -Br, -I, -F, -Me, -OMe, -NO_2, and **1c** and **1d**) and phthalanilic acid itself (**1b**) the predominant reaction in dilute aqueous media is hydrolysis of the amide with the carboxy function exhibiting a catalytic role in the free acid form.

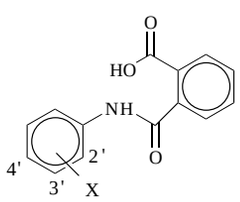

1 X = **a** 2′-NH_2, **b** H, **c** 2′-Me, **d** 2′-Cl

For **1a** the presence of the 2′-amino group induces distinctly anomalous behaviour with hydrolysis being a minor reaction in dilute aqueous acids. The dominant reaction is the formation of *N*-(2-aminophenyl)phthalimide (**B**) (between *ca*. 80 and *ca*. 100% in the pH range studied) and its subsequent rearrangement to 2-(2-carboxyphenyl)benzimidazole (**C**). This is consistent with behaviour previously observed in non aqueous media[1–3] but not with findings for concentrated hydrochloric acid–methanol mixtures[1] or concentrated aqueous sulfuric acid media.[4] Here, little or no **C** is observed and the reaction comprises amide hydrolysis and/or cyclisation to give **B** in varying proportions depending upon the composition of the medium. Cyclisation to the imide has been observed at neutral pH for some *N*-substituted phthalamic acids neutralised with triethylamine in water or aqueous dioxane, followed by distillation.[7] Some imide formation has also been observed during the hydrolysis of *N*-methylphthalamic acid under acidic conditions,[8] but this is a minor reaction contributing to between *ca*. 19 and 35% of the total product in the pH range 0–5. The present study suggests that the anomalous behaviour of **1a** can be linked to amino–carboxy interactions that alter the reaction course. In dilute acid media the sequence of events comprises consecutive pseudo-first-order acid-catalysed processes in the sequence **A** ⟶ **B** ⟶ **C** with a (minor) competing hydrolysis (k_3) reaction of **A** that increases with acid concentration (Scheme 1).

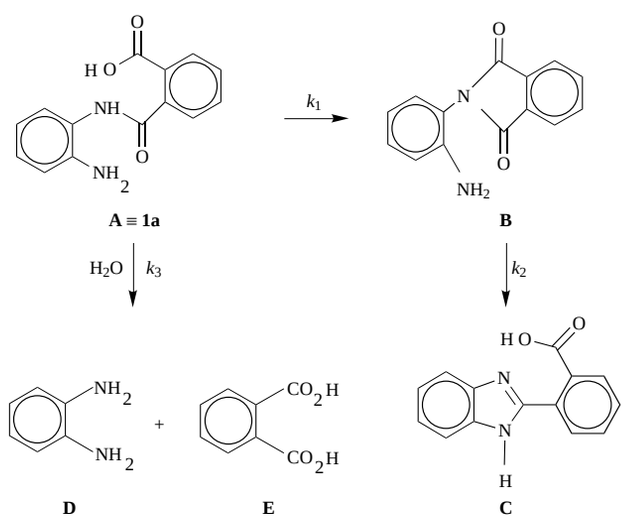

Scheme 1 The competing and consecutive processes observed when *N*-(2-aminophenyl)phthalamic acid (**A**≡**1a**) is subjected to dilute aqueous acid

Results and discussion

Significantly, k_1 and k_2 in Scheme 1 are of comparable magnitude over a wide range of pH so that steady-state kinetics are not applicable. This reaction course is also unusual in proceeding *via* the imide **B** since a range of substituted 2′-aminobenzanilides[5] and 2′-aminoanilides of alkanoic acids,[9] are known to cyclise under acid conditions directly to benzimidazoles without the involvement of kinetically significant intermediates. Hydrolysis of amide in competition with cyclisation is, however, generally observed under high acid concentrations in the examples cited above.

Earlier workers[3,10] have established the presence of some or all of the compounds **A**–**D** in the products from intramolecular reactions of **1a** under a variety of disparate conditions, ranging from aprotic solvents to concentrated aqueous solutions of sulfuric acid. The present study concludes that these products are formed even under dilute aqueous conditions and furnishes a kinetic model for the reactions of **1a** in a wide range of acidic aqueous media. Scheme 1 allows an exact solution to be found

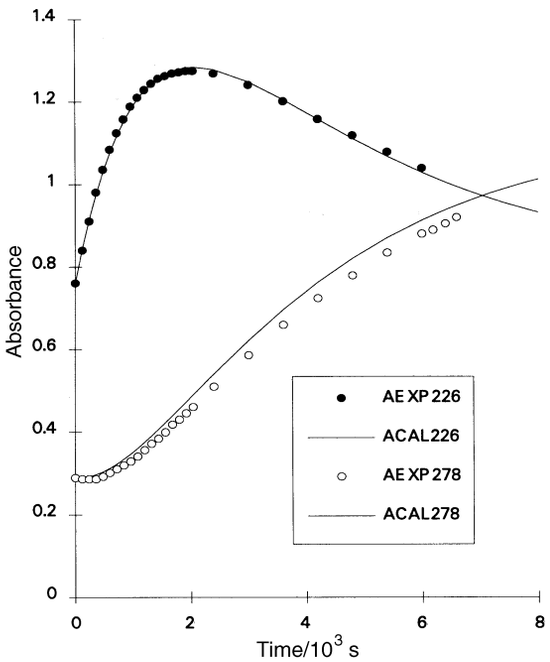

Fig. 1 Experimental (AEXP) and calculated (ACAL) absorbances at 226 and 278 nm for the reaction in Scheme 1 in 0.1 M HCl at 333 K. Both fitted curves are calculated using $k_1 = 7.08 \times 10^{-4}$, $k_2 = 3.15 \times 10^{-4,}$ and $k_3 = 4.52 \times 10–5$ and the relative molar absorptivities given in Table 1.

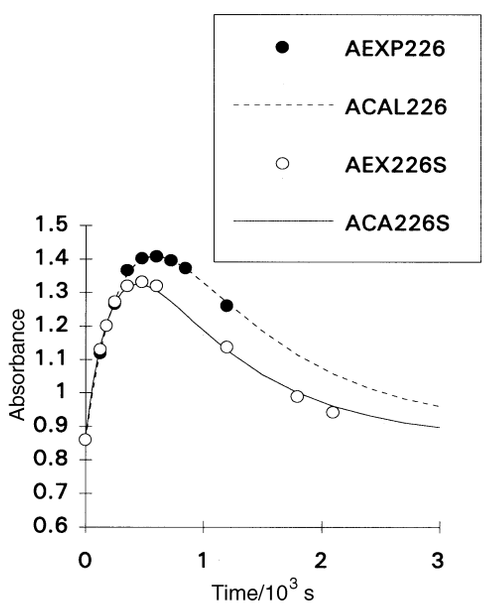

Fig. 2 Absorbance (at 226 nm) *vs.* time plots for the reaction in Scheme 1 comparing the behaviour in 0.1 M HCl (AEXP 226) and 2 M H_2SO_4 (AEXP 226S) at 76.5 °C (349.5 K). The predicted curves (ACALC226 and ACA226S) are calculated from eqns. (1)–(4) using the rate constants in Table 2 . The absorbance values have been corrected to the same initial absorbance (0.86) for direct comparison.

for the concentrations at a given time, *t*, of all the components in the scheme, provided the reaction starts with pure **A** (of concentration $[\mathbf{A}]_0$). The reaction can be conveniently studied by UV spectroscopy with the main areas of change being well separated in wavelength. Consequently, if the molar absorptivities are known, the absorbances due to each component ($A_{\mathbf{A},t}$–$A_{\mathbf{E},t}$) can be calculated using eqns. (1)–(4) (where $\varepsilon_{\mathbf{A}}$–$\varepsilon_{\mathbf{E}}$ are the respective molar absorptivities for each component).

$$A_{\mathbf{A},t} = [\mathbf{A}]_0 e^{-(k_1 + k_3)t} \varepsilon_{\mathbf{A}} \quad (1)$$

Table 1 Relative and absolute values for the molar absorptivities of the component compounds in Scheme 1. Estimates are based on the averages of at least two separate determinations by calculation of the gradient of a best fit line through an absorbance *vs.* concentration plot

	$\varepsilon_{\mathbf{A},rel}$	$\varepsilon_{\mathbf{B},rel}$	$\varepsilon_{\mathbf{C},rel}$	$\varepsilon_{\mathbf{D},rel}$	$\varepsilon_{\mathbf{E},rel}$
Reaction medium	0.1 M HCl				
Wavelength: 226 nm Relative molar absorptivity ($\varepsilon_{\mathbf{A}}$ = 19 440 dm³ mol^{-1} cm^{-1})	1.00	2.36	1.09	0.28	0.41
Wavelength: 278 nm Relative molar absorptivity ($\varepsilon_{\mathbf{A}}$ = 2980 dm³ mol^{-1} cm^{-1})	1.00	0.94	4.09	0.39	0.44
Reaction medium	2.0 M H_2SO_4				
Wavelength: 226 nm Relative molar absorptivity ($\varepsilon_{\mathbf{A}}$ = 20 240 dm³ mol^{-1} cm^{-1})	1.00	2.13	1.09	0.01	0.37
Wavelength: 278 nm Relative molar absorptivity ($\varepsilon_{\mathbf{A}}$ = 3220 dm³ mol^{-1} cm^{-1})	1.00	0.83	3.92	0.05	0.39

Table 2 Values of k_1, k_2 and k_3 (at 349.5 K) in Scheme 1 which give the calculated curves shown in Fig. 2

Medium	$k_1/10^{-3}$ s^{-1}	$k_2/10^{-3}$ s^{-1}	$k_3/10^{-4}$ s^{-1}
0.1 M HCl	2.33	1.12	2.73
2 M H_2SO_4	3.36	1.12	5.89

$$A_{\mathbf{B},t} = \frac{[\mathbf{A}]_0 k_1}{k_2 - k_1 - k_3} [e^{-(k_1 + k_3)t} - e^{-k_2 t}] \varepsilon_{\mathbf{B}} \quad (2)$$

$$A_{\mathbf{C},t} = \frac{[\mathbf{A}]_0 k_1 k_2}{k_2 - k_1 - k_3} \left[\frac{1 - e^{-(k_1 + k_3)t}}{k_1 + k_3} + \frac{e^{-k_2 t} - 1}{k_2} \right] \varepsilon_{\mathbf{C}} \quad (3)$$

$$A_{\mathbf{D},t} + A_{\mathbf{E},t} = \frac{[\mathbf{A}]_0 k_3}{k_1 + k_3} [1 - e^{-(k_1 + k_3)t}] (\varepsilon_{\mathbf{D}} + \varepsilon_{\mathbf{E}}) \quad (4)$$

In practice it was found most convenient to calculate $[\mathbf{A}]_0$ from the initial absorbance for each kinetic run and to use this as the reference for all predicted absorbances.

Two wavelengths (226 and 278 nm) were found to be particularly helpful under most conditions for this study. Changes at 226 nm reflect mainly the change in **B** and those at 278 nm monitor largely the changes in **C**. The consistency of the kinetic model was tested by fitting it to experimental data at 226 and 278 nm keeping the same values for rate constants k_1, k_2 and k_3 at a given temperature. Fig. 1 shows the results for typical experiments at 333 K.

The model was also shown to be valid for the reaction in 2 M sulfuric acid. Here, modified values were used for the molar absorptivities (see Table 1) and significantly increased values for k_3 were required. Fig. 2 shows a comparison for the behaviour of the system at 349.5 K in 0.1 M HCl and 2.0 M H_2SO_4 when studied at 226 nm. The rate constants used to calculate the theoretical curves are summarised in Table 2.

Determination of rate constants

As all of the components of Scheme 1 can be isolated, an opportunity exists to make a separate study of the second consecutive reaction (*i.e.* **B** ⟶ **C**) and independent estimates of k_2 can be made. Values of k_1 and k_3 must be determined indirectly using pre-determined values of k_2.

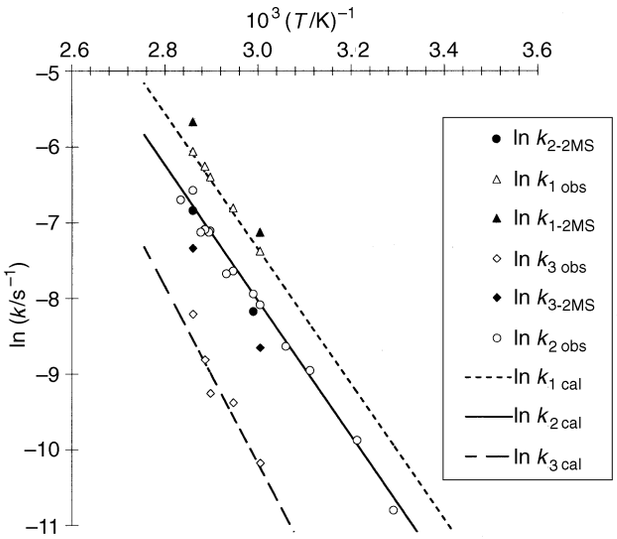

Fig. 3 Arrhenius plots of the observed values for k_1, k_2 and k_3 in Scheme 1. Values for k_2 were determined from the direct study of **B**→**C** (Scheme 1) and those for k_1 and k_3 were determined by fitting the sum of eqns. (1)–(4) to the experimental absorbance *vs.* time plots using non-linear regression analysis methods. The subscripts used are as follows: obs = observed values in 0.1 M HCl, −2MS = observed values in 2 M sulfuric acid, cal = calculated line using: k_1 = e{[−74370.3/(RT)] + 19.489)}, k_2 = e{[−74554.9/(RT)] + 18.870} and k_3 = e{[−97734.9/(RT)] + 25.074}.

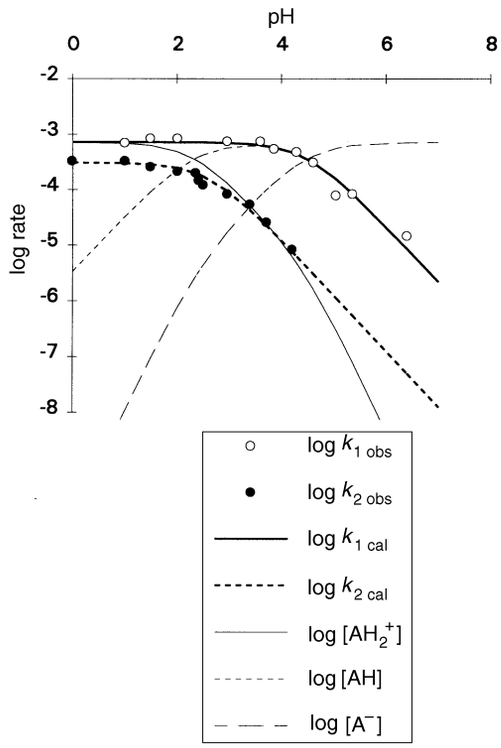

Fig. 4 The pH *vs.* $\log_{10}$ rate profiles for k_1 ($\log k_{1obs}$) and k_2 ($\log k_{2obs}$) at 334.5 K. The curves are drawn from eqns. (9) and (8) and (10) respectively, using the following constants: $K_{a1} = 4.68 \times 10^{-3}$ M (amino function), $K_{a2} = 3.24 \times 10^{-5}$ M (carboxylic function), $K_{a4} = 245 \times 10^{-3}$ M, $K_{a6} = 500$ M, $k_{cat} = 63\ s^{-1}$, $k_1 = k_1' = 7.18 \times 10^{-4}\ s^{-1}$. Superimposed are the calculated values of $\log_{10}$ [$\mathbf{AH_2^+}$], $\log_{10}$ [**A**H] and $\log_{10}$ [$\mathbf{A}^-$].[13] For convenience of scale, $\mathbf{A}_{tot} = 1$ M and the values of the superimposed functions are multiplied by the appropriate rate constants in accordance with eqn. (9). Rate constants are given the values $k_1 = k_1' = 7.18 \times 10^{-4}\ s^{-1}$, the observed plateau value for k_{1obs}.

It was discovered that k_2 is remarkably insensitive to acid concentration in the range 0.1 M HCl to 2 M H_2SO_4. To illustrate the constancy of k_2 over this range of acidity at 334 K, values of $(3.4 \pm 0.1) \times 10^{-4}\ s^{-1}$ were observed in 0.1 and 1.0 M HCl, and in 2 M H_2SO_4 and 1 M acetic acid, values of $(2.8 \pm 0.1) \times 10^{-4}\ s^{-1}$ were determined (see also Fig. 3).

Method 1 makes use of the observation that, by coincidence, at 226 nm, the initial and final absorbances are very similar provided the pH is between 1 and 2. This approximation becomes less valid (but still useful) as the acid concentration increases owing to the increasing significance of k_3. Consequently, over a range of acid concentrations, $[\mathbf{B}]_{max}$ occurs at a time very close to A_{max}, allowing reasonably accurate estimates of t_{max} . This permits the determination of values for ($k_1 + k_3$) by iterative methods using eqn. (5) and an appropriate value of

$$t_{max} = \frac{\ln[(k_1 + k_3)/k_2]}{k_1 + k_3 - k_2} \quad (5)$$

k_2. Provided that $k_3 < k_1$ (and therefore $A_0 \approx A_\infty$), $[\mathbf{B}]_{max}$ can be estimated from A_{max} using the data in Table 1. $[\mathbf{B}]_{max}$ is defined as eqn. (6) which when rearranged to eqn. (7), allows the evaluation of k_1, and thereby k_3.

$$[\mathbf{B}]_{max} = \frac{k_1[\mathbf{A}]_0}{k_2 - k_1 - k_3}\left[e^{-(k_1+k_3)t_{max}} - e^{-k_2 t_{max}}\right] \quad (6)$$

$$k_1 = \frac{[\mathbf{B}]_{max}[k_2 - (k_1 + k_3)]}{[e^{-(k_1+k_3)t_{max}} - e^{-k_2 t_{max}}][\mathbf{A}]_0} \quad (7)$$

Method 2 evaluates the rate constants using non-linear regression analysis to fit eqns. (1)–(4) to the experimental data. Results from either method gave acceptable agreement from a given set of data (Table 3), but levels of confidence by either method can be summarised as $k_2 > k_1 \gg k_3$, with method 2 being more reliable at higher acid concentrations. Estimates of the ratio k_3/k_1 under a range of conditions are summarised in Table 4.

Variation of rate constants with temperature and mineral acid concentration

Separate studies were made using pure **B** as the starting material to investigate the variation in k_2 with both parameters. A good Arrhenius relationship was observed (Fig. 3) and since k_2 proved so insensitive to mineral acid concentration it was decided to use the same calculated value for k_2 in 0.1 M HCl and 2 M H_2SO_4, at a given temperature, to estimate k_1 and k_3. Fig. 3 summarises these results and allows E_{act} to be estimated as 74.4, 74.6 and ~98 kJ mol^{-1}, respectively, for the reactions represented by k_1, k_2 and k_3. Values for $\Delta S^\ddagger$ are −90, −95 and ~−44 J mol^{-1} K^{-1}, respectively. However, if estimated k_{cat} values (see Scheme 2) for the 'true' unimolecular catalysed reaction are used instead of observed pseudo-first-order rate constants, $\Delta S^\ddagger$ has a value of *ca.* +15 J mol^{-1} K^{-1} for the reaction **B** ⟶ **C** (k_2), a value which is much more consistent with an intramolecular process. The values of k_{cat} can be estimated from k_{obs} using eqn. (8) and the parameters (K_{a1}, K_{a2}, K_{a4}, and K_{a6}) given for Fig. 4.

$$k_{2,obs}[\mathbf{B}]_{tot} = k_{cat}[\mathbf{J}] = k_{cat}[\mathbf{B}]_{tot}\left[\frac{[H^+]K_{a4}}{([H^+] + k_{a4})([H^+] + K_{a6})}\right] \quad (8)$$

The data presented in Fig. 3 and Table 4, clearly show the suppressed rate of hydrolysis over cyclisation for **1a**. Hawkins'[6] data shows that at 333 K phthalanilic acid (**1b**), has a pseudo-first-order rate constant for hydrolysis of *ca.* $5 \times 10^{-3}\ s^{-1}$. When compared with the estimate of *ca.* $4 \times 10^{-5}\ s^{-1}$ for k_3 this shows the 2-amino group of **1a** suppresses hydrolysis by a factor of *ca.* 125. This comparison also rules out any likelihood of intramolecular acid catalysis of hydrolysis by NH_3^+ in **1a**, since

Table 3 A comparison of some estimates of the values of k_1 and k_3 (at 349.5 K), using Methods 1 and 2

	Method 1		Method 2	
Medium	$k_1/10^{-3}$ s^{-1}	$k_3/10^{-4}$ s^{-1}	$k_1/10^{-3}$ s^{-1}	$k_3/10^{-4}$ s^{-1}
0.1 M HCl	2.16	1.87	2.33	2.73
2 M H_2SO_4	3.31	4.94	3.36	5.89

NH_3^+ should be at least as effective a catalyst (from pK_a values) as carboxylic acid[6] and can be shown by simple modelling to have similar 'intramolecular access' to the amide function. Ring closure of **1a** to the imide ($k_1 \approx 7 \times 10^{-4}$ s^{-1} at 333 K), being slower than hydrolysis of **1b** by a factor of *ca*. 7.5, also indicates a suppression of hydrolysis rather than simply an increase in the rate of imide formation. This evidence suggests that the carboxy group and protonated amino functions in **1a** are being prevented from acting as intramolecular catalysts for hydrolysis. This argument is supported by pK_a measurements which are discussed later.

Variation of rate constants with pH

At low mineral acid concentrations (below 0.1 M HCl) the magnitudes of ($k_1 + k_3$) and k_2 were determined in buffer solutions of known pH. The sensitivity to ionic strength and buffer concentrations were both demonstrably small and so the system was analysed in terms of specific acid catalysis, ignoring the small contributions from general acids. Also in the range studied, k_3 was assumed to be insignificant compared with k_1 and so the assumption ($k_1 + k_3$) $\approx k_1$ was applied, allowing estimates for k_1 with an accuracy of *ca*. ±5%. At pH values greater than the pK_a of **B**, (*ca*. 2.61), significant spectral changes prevent the use of methods 1 and 2 above. Instead, the rise in absorbance at 290 nm (corresponding to increasing **B**) was used to determine k_1 directly. In this region, k_2 is <10% of k_1 resulting in approximately first-order behaviour for the observed changes in **B**, allowing a satisfactory estimation of k_1. Fig. 4 shows the observed pH *vs*. rate profiles and Schemes 2 and 3 show proposed mechanisms (1 & 2) for the processes associated with k_1 and k_2.

Table 4 Comparison of some estimates of k_1/k_3 by various methods

	Method 1	Method 2	Product analysis[a]	Product analysis[b]
0.1 M HCl	11.5	8.5	13	—
2 M H_2SO_4	6.7	5.7	3	—
1 M DCl–D_2O	—	—	—	9

[a] Gravimetric determination of *o*-phenylenediamine (**D**) by solvent extraction. [b] *In situ* 270 MHz ^{1}H NMR determination.

Mechanism 1

At a given pH, the values of [**A**$^-$], [**A**H] and [**A**H$_2^+$] in Scheme 2 can be calculated from published expressions.[11] The observed rate for the process described in Mechanism 1 (Scheme 2) can be shown by the steady-state approximation given in eqn. (9), where [$\mathbf{A}_{tot}$] = [**A**H$_2^+$] + [**A**H] + [**A**$^-$].

$$\frac{-\mathrm{d}[\mathbf{A}]_{tot}}{\mathrm{d}t} = k_{1obs}[\mathbf{A}_{tot}] = k_1[\mathbf{A}H_2^+] + k_1'[\mathbf{A}H] + 0[\mathbf{A}^-] \quad (9)$$

Observed behaviour requires that $k_1 \approx k_1'$ in eqn. (9) in order to explain the transition from [**A**H$_2^+$] to [**A**H] as the kinetically significant species without a change in the value of k_{1obs}. If $k_1 = k_1'$, then eqn. (9) rearranges to give eqn. (10). The equivalence of k_1 and k_1' is unexpected, but can be rationalised if it is accepted that the change in protonation state of the amino function of **A** is accompanied by two self cancelling phenomena. Protonation of the amino function in **A** (pK_a = 2.33 by titrimetric methods; *cf*. 2.61 for the amino group in **B** by kinetic methods) will simultaneously enhance the intramolecular catalysis of amide attack at the carbonyl group, and reduce (by inductive effects) the nucleophilicity of the amide nitrogen. If these opposing changes exert effects of similar magnitude, then a significant change in rate will only be observed when the

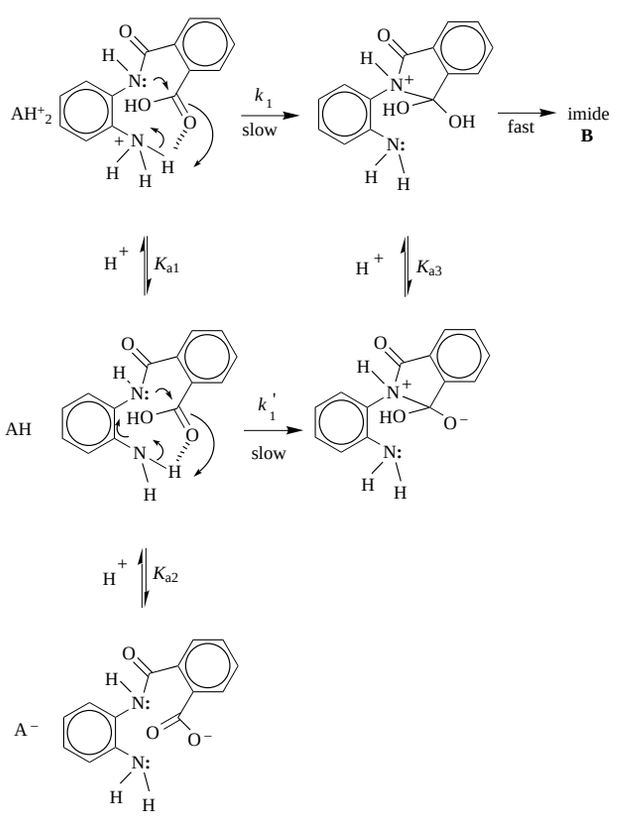

Scheme 2 Mechanism 1: the proposed mechanism for the processes associated with the observed k_1 in Scheme 1

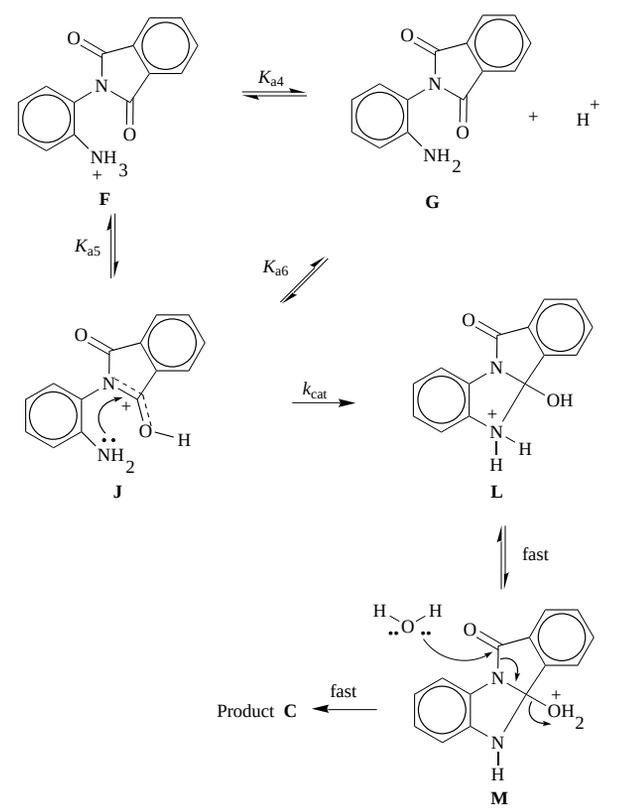

Scheme 3 Mechanism 2: the proposed mechanism for the processes associated with the observed k_2 in Scheme 1

amino–carboxy 'complex' (Scheme 2) is disrupted by deprotonation of the COOH function. This provides indirect evidence for strong associations between the carboxy and amino functions without which it is difficult to explain the independence of k_{1obs} with regard to amino group titration in **A**. Comparison of the carboxylic pK_a for **A** (4.43 by titrimetric methods, 4.49 by kinetic methods) with published values[6,12] for that of phthalanilic acid (**1b**, pK_a = 3.62) indicates that in **A**, the carboxy function has considerably diminished acidity, again pointing to 'proton trapping'. (Note that the two cited values for the pK_a of the carboxy function in phthalanilic acid in refs. 6 and 12 are in good agreement and at considerable odds with a third value found[13] of 4.35.) Fig. 4 shows how the calculated concentrations of [**A**H_2^+], [**A**H] and [**A**$^-$] in Scheme 2 vary with pH. Superimposition of the observed values for k_1 (k_{1obs}) demonstrates how the kinetic significances of [**A**H_2^+] and [**A**H] vary in accordance with eqn. (10).

$$\frac{-\mathrm{d}[\mathbf{A}]_{tot}}{\mathrm{d}t} = k_{1obs}[\mathbf{A}_{tot}] = k_1([\mathbf{A}H_2^+] + [\mathbf{A}H]) \qquad (10)$$

Mechanism 2

Scheme 3 shows the proposed pre-equilibrium species for Mechanism 2 and the suggested path to products. Doubly protonated species have been omitted since they will be expected to be a negligible proportion of total reactant in the pH range studied. Whether structure **M** dehydrates to give 1,2-benzoylenebenzimidazole (11*H*-isoindolo[2,1-*a*]benzimidazol-11-one) (**M** − H_3O^+) as a rapidly hydrolysed intermediate is open to question. The compound was prepared and shown to hydrolyse at 333 K[14] with a rate constant of between *ca*. 10k_2 and *ca*. 100k_2 depending on pH (the rate rising with falling pH), which is broadly in agreement with published values.[15] This data supports the possibility that such an intermediate is formed. Evidence from UV spectra of solutions of **A** in anhydrous acetic acid,[15] strongly suggests the formation of 1,2-benzoylenebenzimidazole and only a slow breakdown to compound **C**, presumably through reaction with water generated during the closure of the two ring systems.

For the rate-determining step in dilute aqueous acid (k_{cat}, Scheme 3), the suggestion is that while the amino function is protonated it cannot be nucleophilic. Since the reaction is clearly acid catalysed, the kinetically significant form is **J**, which, although existing at very low concentration, is highly reactive. The total compound B in solution can be defined as $[\mathbf{B}]_{tot} = [\mathbf{F}] + [\mathbf{G}] + [\mathbf{J}]$. Knowing that $[\mathbf{J}] \ll [\mathbf{B}]_{tot}$ approximations (11) and (12) may be derived, and consequently eqns. (13) and (8).

$$[\mathbf{F}] \approx [\mathbf{B}]_{tot} \frac{[H^+]}{([H^+] + K_{a4})} \qquad (11)$$

$$[\mathbf{G}] \approx [\mathbf{B}]_{tot} \frac{K_{a4}}{([H^+] + K_{a4})} \qquad (12)$$

$$[\mathbf{J}] = [\mathbf{B}]_{tot} \frac{[H^+]K_{a4}}{([H^+] + K_{a4})([H^+] + K_{a6})} \qquad (13)$$

$$k_{2obs}[\mathbf{B}]_{tot} = k_{cat}[\mathbf{J}] = k_{cat}[\mathbf{B}]_{tot} \frac{[H^+]K_{a4}}{([H^+] = K_{a4})([H^+] + K_{a6})} \qquad (8)$$

Fig. 4 shows how eqn. (8) can be used to explain the pH *vs*. rate profile for k_2 in Scheme 1. Theoretically, k_{2obs} should turn down at the pK_a of the imide function as well as that of the amine function with the width of the plateau determined by $pK_{a\ amine} - pK_{a\ imide}$. In practice if $pK_{a\ imide}$ is negative then the turn down with decreasing pH will not be observed under dilute aqueous conditions. Arient and Marham[10], noted that the hydrochloride of **B** quickly cyclises quantitatively to **C** in boiling water and the addition of HCl does not affect the reaction rate; a fact that is consistent with the profile for k_2 in Fig. 4. Furthermore, changing the solvent to methanol effectively prevents benzimidazole formation, as does using concentrated sulfuric acid solvents for **A**,[4] which is consistent with the idea that when the pre-equilibrium in Scheme 3 supports vanishingly small concentrations of **J** and the formation of **C** is suppressed.

Eqn. (8) can be easily fitted to the experimental data, but the accuracy of k_{cat} is dependent upon the values used for the equilibrium constants. For the amino function, K_{a4} can be estimated from the kinetic data (pK_a = 2.60). Very few experimentally determined literature values for pK_a (**B**H$^+$) of imide functions have been published and suitable values for **B** have not been found. No major changes in the UV spectrum of **B** have been observed on changing from 0.1 M HCl to 2 M H_2SO_4 suggesting that a value < 0 is most likely. Hawkins[6] quotes a value of −2.7 for the amide function in phthalanilic acid (**1b**) and this was taken as an acceptable model putting K_{a6} in the region of 500 M. This allows an estimation for k_{cat} of *ca*. 63 s^{-1}.

The model presented for mechanism 2 can be generally applied to other analogous reactions involving the acid-catalysed attack of an amino group on a relatively unreactive carbonyl group, such as an amide. In these cases, unlike oxime formation, for example, the uncatalysed reactions are very slow due to the unreactive nature of the modified carbonyl group. A good example is the acid-catalysed cyclisation of *N*-(2-aminophenyl)ethanamide (*o*-aminoacetanilide) to give 2-methylbenzimidazole, studied by Morgan and Turner.[9] The pH rate profile in the range 0–6 is remarkably similar to that for k_2 in Fig. 4 . Morgan and Turner discuss the apparent contradiction of a protonated amino function increasing the rate of nucleophilic attack at an amide carbonyl in terms of intramolecular general acid catalysis by $-NH_3^+$. An alternative explanation is to use the model proposed in Scheme 3 with K_a imide (K_{a5}) substituted by $K_{a\ amide}$ for *o*-aminoacetanilide. Morgan's data shows an apparent decrease in rate in the pH 0–1 region, which is not discussed. When fitted to eqn. (8) (using the given value[9] of $pK_{a\ amine}$ = 3.2) *a* $pK_{a\ amide}$ of ~0.0, and a $k_{cat} \approx 0.1$ s^{-1} emerge at 323 K. For comparison, the pK_a values of amide functions in acetamide[17] (0.63), phthalamic acid[16] (−2.5) and phthalanilic acid[6] (−2.7) suggest that a value of ~0 is not unreasonable for *o*-aminoacetanilide. Published values of pK_a (**B**H$^+$) for substituted acetanilides[18] show a range of *ca*. −0.8 to −2.3 with acetanilide at −1.43. The general trend is that the more electron donating the ring substituent, the more pK_a tends to zero. It is important to stress that in the proposed Scheme (Scheme 3), the discounting of doubly protonated species means that the basicity of species **J** (and its analogue in the cyclisation of *o*-aminoacetanilide), will be influenced by 2′-NH_2 and not 2′-NH_3^+, again indicating that for *o*-aminoacetanilide, the relevant amide pK_a is ~0. A value of k_{cat} = 0.1 s^{-1} for *o*-aminoacetanilide cyclisation, points to a unimolecular rate-determining step that is significantly less efficient than for **B** (*ca*. 300 times slower) even after allowing for temperature differences.

Experimental

Preparation of materials

***N*-(2-Aminophenyl)phthalamic acid (1a≡A).** This compound was prepared by two different methods.

Method A.—Freshly recrystallised ($CHCl_3$) phthalic anhydride (14.8 g) was dissolved in cold chloroform (200 cm^3) with stirring. A solution of freshly recrystallised ($CHCl_3$) 1,2-diaminobenzene in boiling chloroform (200 cm^3) was also prepared. The amine solution was removed from the heat source and the temperature recorded as 60 °C. Then the anhydride solution was added in 20 cm^3 aliquots with thorough stirring between additions. The final temperature was recorded as 45 °C

and the mixture was allowed to stand overnight. The crude product (19.0 g, 74%) was vacuum filtered and washed well with diethyl ether and air dried to constant weight. Recrystallisation was carried out by dissolving the total product in boiling methanol (125 cm^3), treating it with activated charcoal and allowing the filtrate to cool to room temperature by standing for 2 h. Purified material (5.5 g, mp 149–152 °C with decomposition) was recovered by vacuum filtration and air drying. Further material (4.5 g) was recovered by increasing the filtrate volume to 250 cm^3 with diethyl ether and standing the solution overnight at room temperature.

Method B.—Crude product was obtained by reacting phthalic anhydride and 1,2-diaminobenzene (0.2 mol of each) in DMF according to the procedure of Young.[2] This material was then further purified from methanol as described in Method A above. Literature melting points given are 147°–150 °C[2] and 151–152 °C.[19] Analysis, found: C, 65.78; H, 4.4; N, 10.83. Calc. for $C_{14}H_{12}N_2O_3$: C, 65.62; H, 4.72: N, 10.93%.

***N*-(2-Aminophenyl)phthalimide (B).** Dilute 2 M HCl (20 cm^3) was heated to 65–70 °C in a 50 cm^3 conical flask with magnetic stirring. Solid *N*-(2-aminophenyl)phthalamic acid (1.30 g) was added directly to the flask and stirring continued until a clear solution was obtained. After a few minutes more stirring, a white precipitate appeared and after 8 min ice was added to bring the temperature to 25 °C. The white solid was either filtered off as the hydrochloride of *N*-(2-aminophenyl)-phthalimide (0.50 g, 33.5%, mp 240–245 °C, lit.,[10] values 253–255 °C and 272 °C), or neutralised in suspension with 0.880 M aqueous NH_3 to give a yellow solid which was *N*-(2-aminophenyl)phthalimide (0.30 g, 33.1%, mp 182–4 °C, lit.,[2] 194–195 °C). For kinetic work the crude compound was recrystallised from ethanol to give material with a melting point of 192–193 °C. Analysis, found: C, 70.29; H, 4.05; N, 11.54. Calc. for $C_{14}H_{10}N_2O_2$: C, 70.58; H, 4.23; N, 11.76%.

1,2-Benzoylenebenzimidazole (11*H*-isoindolo[2,1-*a*]benzimidazol-11-one). *N*-(2-Aminophenyl)phthalamic acid (2.0 g) was placed in a 100 cm^3 beaker and heated to its melting point on an electric hotplate. The temperature was gradually raised until sublimation occurred and the product was collected by closing the beaker with a glass petri-dish cooled by standing a small flask of cold water on top of it. Bright yellow needles of 1,2-benzoylenebenzimidazole (0.80 g, 46.5%, mp 215–220 °C, lit.,[2] 214–215 °C) were collected in this way.

2-(2-Carboxyphenyl)benzimidazole (C). *N*-(2-Aminophenyl)-phthalamic acid (**1a**≡**A**, 10.0 g) was refluxed for 1.5 h in 1 M aqueous HCl (100 cm^3). The solution was then cooled to room temperature and neutralised with 0.880 M aqueous NH_3, whereupon a white solid was precipitated. The mixture was allowed to stand at room temperature overnight before the crude product (6.5 g, 70%) was filtered under vacuum and washed with water before drying. Pure material (mp 262–263 °C) was obtained by repeated recrystallisation of small samples from ethanol. Note, considerable variation in reported mp has been observed (*cf.* 245 °C,[2] 271.5 °C[10] and 270 °C[20]). Analysis, found: C, 70.37; H, 4.01; N, 11.51. Calc. for $C_{14}H_{10}N_2O_2$: C, 70.58; H, 4.23; N, 11.76.

Buffer solutions

All mineral acid solutions (0.1 M HCl and 2 M H_2S0_4) were prepared from AnalaR grade materials and other buffer solutions (citric acid–Na_2HPO_4) were prepared directly from McIlvaine's table of Standard Buffers.[21] All pH values were checked before use by employing a glass electrode and were found to be as stated in the table (±0.1). Where buffer dilution experiments were conducted, the stock buffers (HCl–KCl, acetic acid–acetate and formic acid–formate) were made to a total ionic strength of 0.1 M and a series of dilutions made with 0.1 M KCl. Again, the pH was measured before use.

Kinetic measurements

All kinetic work was carried out using a Perkin Elmer λ 5 double beam UV–VIS spectrophotometer with a water heated sample cell and the appropriate reaction medium in the reference cell. A flow of heated water was maintained with a Grant thermostatted heater and pump operating in a separate bath. Temperatures (±0.2 °C) were determined by direct measurement of the cuvette contents using a thermocouple and cross checks made with a mercury thermometer. Each run was conducted in a conventional 1 cm stoppered quartz cuvette containing *ca*. 2.5 cm^3 of solution. Cuvettes containing the reaction solvent were allowed to equilibrate for at least 10 min in the spectrometer before the addition of reactant. Reactants were introduced to the cuvettes by preparing saturated solutions of the compounds in absolute ethanol at room temperature and then adding an appropriate volume (typically 10–50 μl) to give the required initial absorbance. Cuvettes were stoppered and rapidly inverted 2–3 times before data collection was started. The wavelength used was dependent on the pH of the buffer employed in the study and this is made clear in the discussion. At each pH the appropriate wavelength was determined from a full spectrum of both product(s) and reactant.

Acknowledgements

The author thanks the Royal Society of Chemistry for a personal research grant that has made much of the kinetic work possible. Thanks are also due to Martin Gilligan, Sartaj Kahlon, Maniha Gul, Maria Rodruigez-Sol and Kath Shelley.

References

1 J. Arient, *Russ. Chem. Rev.* (*Engl. Transl.*), 1965, **34**, 836.
2 P. R. Young, *J. Heterocycl. Chem.*, 1972, **9**, 371.
3 V. V. Korshak, A. L. Rusanov and R. D. Katsarava, *Vysokomol. Soedin., Ser. A*, 1972, **14**, 1917.
4 V. K. Shchel'tsyn, M. I. Vinnick, E. A. Sycheva and G. S. Krasil'nikova, *Kinet. Catal.* (*Engl. Transl.*), 1990, **31**, 970.
5 V. K. Shchel'tsyn, M. I. Vinnick, E. A. Sycheva and G. S. Krasil'nikova, *Kinet. Catal.* (*Engl. Transl.*), 1989, **30**, 914.
6 D. Hawkins, *J. Chem. Soc., Perkin Trans. 2*, 1976, 642.
7 E. Hoffmann and H. Schiff-Shenav, *J. Org. Chem.*, 1962, **27**, 4686.
8 J. Brown, S. C. K. Su and J. A. Shafer, *J. Am. Chem. Soc.*, 1966, **88**, 4468.
9 K. J. Morgan and A. M. Turner, *Tetrahedron*, 1969, **25**, 915.
10 J. Arient and J. Marhan, *Collect. Czech. Chem. Commun.*, 1961, **26**, 98.
11 See for example: C. A. Reynolds, *Principles of Analytical Chemistry*, Allyn and Bacon, 1966, pp. 60–61.
12 H. Morawetz and J. A. Shafer, *J. Am. Chem. Soc.*, 1962, **84**, 3783.
13 C. L. Sharma, R. S. Arya, S. S. Narvi and V. Mishra, *J. Indian. Chem. Soc.*, 1984, **61**, 677.
14 S. Kahlon, B.Sc. Project Report, University of Wolverhampton, 1994.
15 M. Gul, B.Sc. Project Report, University of Wolverhampton, 1994.
16 M. L. Bender, Y.-L. Chow and F. Chloupek, *J. Am. Chem. Soc.*, 1958, **80**, 5380.
17 *Organic Chemistry Data Book* (S246DB), The Open University, 1991, p. 7.
18 C. J. Giffney and C. J. O'Connor, *J. Chem. Soc., Perkin Trans. 2*, 1975, 706.
19 J. G. Colson, R. H. Michel and R. M. Paufler, *J. Polym. Sci., Polym. Chem. Ed.*, 1966, **4**, 59.
20 P. N. Preston, *The Chemistry of Heterocyclic Compounds, Part 1*, Wiley-Interscience, 1981, vol. 40, p. 239.
21 *Handbook of Chemistry and Physics*, eds. C. D. Hodgman, R. C. Weast and S. M. Selby, Chemical Rubber Publishing Company, Cleveland, OH, 39th edn, 1957, p. 1615.

Paper 6/06699B
Received 30*th September* 1996
Accepted 14*th January* 1997